

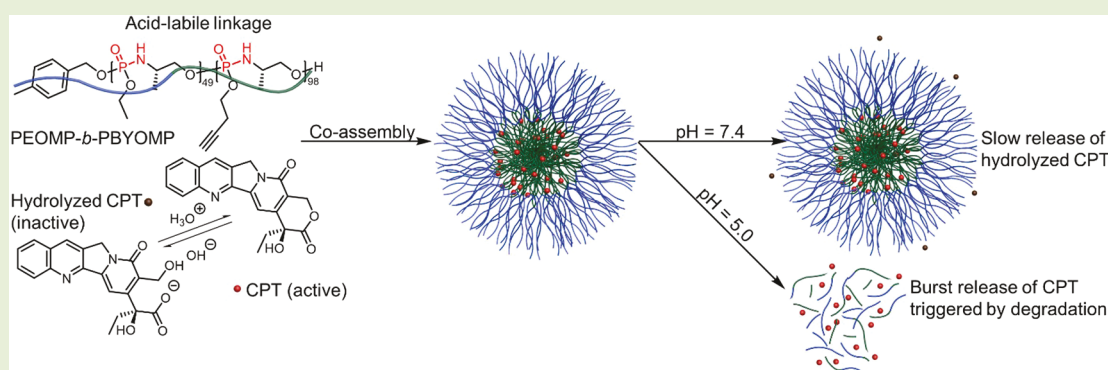
Acid-Triggered Polymer Backbone Degradation and Disassembly to Achieve Release of Camptothecin from Functional Polyphosphoramidate Nanoparticles

Hai Wang,[†] Mei Dong,[†] Sarosh Khan,[†] Lu Su,[†] Richen Li,[†] Yue Song,[†] Yen-Nan Lin,[†] Nari Kang,[†] Christopher H. Komatsu,[†] Mahmoud Elsabahy,^{†,‡} and Karen L. Wooley^{*,†}

[†]Departments of Chemistry, Chemical Engineering, and Materials Science & Engineering, Laboratory for Synthetic–Biologic Interactions, Texas A&M University, College Station, Texas 77842, United States

[‡]Department of Pharmaceutics, Faculty of Pharmacy, Assiut University, Assiut 71515, Egypt

Supporting Information



ABSTRACT: Camptothecin (CPT) is a promising anticancer drug, yet its therapeutic potential has been limited by poor water solubility and facile hydrolysis of the lactone form into an inactive carboxylate form at neutral pH. In this work, a fundamental synthetic methodology was advanced to allow for the preparation of well-defined functional polyphosphoramidate (PPA)-based block copolymers that coassembled with CPT into nanoparticles, which underwent coincident acid-triggered polymer backbone degradation, nanoparticle disassembly, and CPT release. Encapsulation of CPT by the PPA polymer inhibited premature hydrolysis of CPT at pH 7.4 and enabled accelerated CPT release at pH 5.0 (ca. 4× faster than at pH 7.4). Two degradable oxazaphospholidine monomers, with one carrying an alkyne group, were synthesized to access well-defined block PPAs (dispersity, $\bar{D} < 1.2$) via sequential organobase-catalyzed ring-opening polymerizations (ROP). The resulting amphiphilic block copolymers (PEOMP-*b*-PBYOMP) were physically loaded with CPT to achieve well-dispersed nanotherapeutics, which allowed the aqueous suspension of CPT at concentrations up to 3.2 mg/mL, significantly exceeding the aqueous solubility of the drug ($< 2.0 \mu\text{g/mL}$ at 37 °C). Cytotoxicity studies revealed enhanced efficacy of the CPT-loaded nanoparticles over free CPT in cancer cells and similar toxicity in normal cells.

Polymeric systems with the ability to respond to external stimuli, including pH,¹ light,² temperature,^{2,3} redox,⁴ electric fields,⁵ etc., have great potential for biomedical applications. By taking advantage of such systems, strategies are being pursued to achieve triggered drug release preferentially at pathological sites to lead to higher accumulation of drug in the targeted disease sites and, thus, enhanced efficacy and decreased side effects.⁶ For instance, the higher concentration of glutathione in cancer cells has been extensively exploited to achieve triggered release of therapeutics from reduction-responsive carriers.⁷ Similarly, the lower pH of cancer and inflammation microenvironments has led to numerous elegant pH-responsive systems.^{7d,e,8}

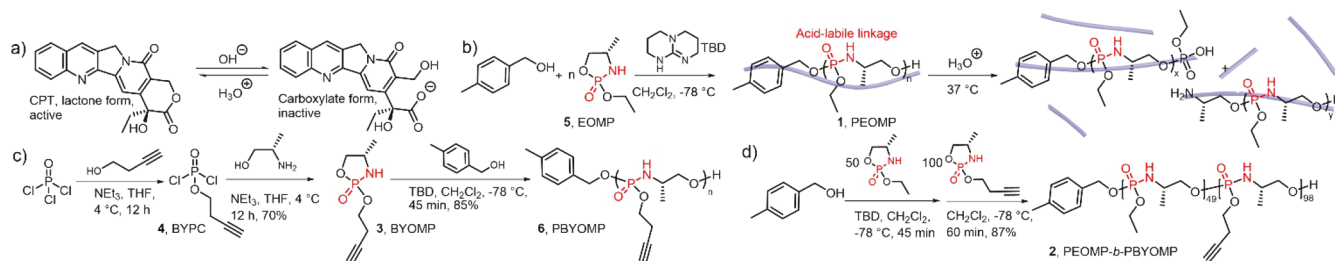
Camptothecin (CPT), a topoisomerase II inhibitor discovered from the Chinese tree *Camptotheca acuminata* over half a

century ago, would benefit greatly from such systems, due to the facile hydrolysis of its therapeutically active lactone form into an inactive carboxylate form at physiological pH (Scheme 1a) and low aqueous solubility ($< 2.0 \mu\text{g/mL}$ at 37 °C).⁹ In the past several decades, a variety of responsive polymeric systems have been developed to improve the therapeutic efficacy of CPT, among which two major strategies were applied: (1) conjugation of CPT onto polymeric systems through acid/reduction-labile linkages¹⁰ and (2) physical encapsulation of CPT into an acid/reduction-responsive polymeric system.¹¹ Generally, the first strategy requires more synthetic steps and

Received: May 14, 2018

Accepted: June 11, 2018

Scheme 1. (a) Hydrolysis of CPT, (b) Polymerization of EOMP, **5**, to Afford PEOMP, **1**, with Acid-Triggered Backbone Degradation, (c) Synthesis and Polymerization of BYOMP, **3**, to Afford Alkyne-Functionalized Polyphosphoramidates, PBYOIMP, **6**, and (d) One-Pot Sequential Polymerization of **5** and **3** to Afford the Amphiphilic Diblock Copolymer PEOMP-*b*-PBYOIMP, **2**



has less versatility for adaption to other therapeutics; nevertheless, it effectively inhibits the premature release and hydrolysis of CPT. In contrast, the second strategy requires less synthetic effort and is more versatile; however, the premature release of CPT is often unavoidable. As such, highly responsive systems are desired to facilitate cancer-cell-specific delivery of therapeutically active CPT.

Introduction of acid-labile linkages along a polymer backbone is anticipated to lead to rapid acid-triggered degradation, given that even slight degradation of the backbone would markedly decrease molar mass.¹² In an earlier study, we demonstrated that the polyphosphoramidate (PPA) poly(4*S*-2-ethoxy-4-methyl-1,3,2-oxazaphospholidine 2-oxide) (PEOMP, **1**) was highly water-soluble (>800 mg dissolved in 1 mL of water) and that it was able to undergo accelerated degradation under acidic conditions, due to the presence of acid-labile phosphoramidate linkages along the backbone (Scheme 1b).¹³ With an interest in expanding this PPA backbone chemistry to hydrophobic polymer blocks and amphiphilic block copolymers that also carry reactive functionalities, we developed a synthetic route to a well-defined amphiphilic diblock copolymer, PEOMP-*b*-PBYOIMP, **2**, with acid-labile linkages along the backbone. This block copolymer was afforded via a novel oxazaphospholidine monomer bearing a side-chain alkyne functionality upon controlled one-pot sequential organobase-catalyzed ring-opening polymerizations (ROPs) and required no further chemical modification to exhibit amphiphilic character (Scheme 1d). Coassembly of **2** with CPT in aqueous solutions yielded nanotherapeutics, which were evaluated *in vitro* and revealed enhanced efficacy over free CPT in cancer cells and similar toxicity in normal cells.

The monomer, (4*S*)-2-(but-3-yn-1-yloxy)-4-methyl-1,3,2-oxazaphospholidine 2-oxide (BYOMP, **3**), was synthesized by annulation of but-3-yn-1-yl phosphorodichloridate (BYPC, **4**) with (*S*)-(+)-2-amino-1-propanol in the presence of triethylamine (Scheme 1c). Addition of but-3-yn-1-ol to phosphorus(V) oxychloride yielded **4**, which was initially purified by vacuum distillation prior to use in monomer synthesis. However, given that the reaction proceeded quantitatively, as evidenced by only the peak of **4** at 7.55 ppm being observed in the ³¹P NMR spectrum, annulation reactions were then conducted with crude **4**. Notably, the use of crude **4** afforded little reduction of the yield of **3** and substantially increased the overall yield of the two reactions from 29% to 70%. The annulation reaction was highly efficient, and purification was accomplished simply by filtration through a silica gel plug to remove the slight excess of triethylamine to give **3** as a highly viscous colorless liquid. The purity of **3** was confirmed by mass

spectrometry. The ³¹P NMR spectrum of **3** showed resonances at 25.62 and 24.85 ppm, similar to the ³¹P chemical shift values reported for EOMP (25.97 and 25.20 ppm), **5**,¹³ and other cyclic phospholane amidate structures.¹⁴ The two distinct resonances were attributed to diastereomers formed during the annulation. The ¹H and ¹³C NMR spectra of the monomer also showed two sets of resonance frequencies corresponding to the two diastereomers. Resonances in the ¹H NMR spectrum were able to be distinguished through homonuclear correlation spectroscopy (COSY) (Figure S1), and the intensities of the 4-methyl proton resonances at 1.23 and 1.29 ppm, respectively, revealed the two diastereomers to be present at roughly equal proportions in the mixture (45:55).

Conditions to allow for controlled ROP of **3** were then investigated. Initially, the polymerization was conducted in the presence of the organocatalyst 1,8-diazabicyclo[5.4.0]undec-7-ene (DBU), which had previously provided excellent control of the ROP of cyclic carbonate and cyclic phosphotriester monomers.¹⁵ However, similarly as observed in the ROP of **5**,¹³ DBU failed to yield appreciable conversion of **3** to polymer in dichloromethane (DCM), even at relatively high catalyst loadings (10 mol % relative to monomer). Thus, DBU was replaced by the more active catalyst 1,5,7-triazabicyclo[4.4.0]dec-5-ene (TBD), which has successfully mediated the controlled ROP of several cyclic phosphorus-containing monomers.^{13,15c,16} Using a TBD loading of 2 mol % with respect to monomer and 4-methylbenzyl alcohol as the initiator, ROP of **3** in DCM was studied, monitoring monomer conversion and the growth of polymer chains as a function of time by NMR spectroscopy and *N,N*-dimethylformamide size exclusion chromatography (DMF SEC). Monomer conversions were obtained from ³¹P NMR spectra on aliquots taken from the polymerization mixtures. Subsequently, number-average molar masses (*M_n*) were calculated from the ¹H NMR spectra after isolation of the polymers by precipitation from dichloromethane into diethyl ether, by comparison of the intensities of the 4-methyl protons originating from the initiator on the α -chain end resonating at 2.34 ppm with the methylene protons adjacent to the alkyne on the repeating units resonating at 2.58 ppm. Molar mass distribution (dispersity, *D*) was measured by DMF SEC calibrated using polystyrene standards. At 0 °C, the polymerization proceeded to 94% conversion within 5 min (entries 1–3, Table 1). However, broadening of *D* (1.2–1.3) was observed at conversions exceeding 75%, indicating the occurrence of adverse backbiting or transesterification reactions. Hence, the reaction temperature was decreased to –78 °C (entries 4–6, Table 1). At this reduced temperature, the polymerization reached >90% conversion within 30 min, and a

Table 1. Polymerization of BYOMP Catalyzed by TBD under Different Conditions^a

entry	T (°C)	[M]/[I]	conv. ^b	M _{n, NMR} ^c (kDa)	Đ ^d	time (min)
1	0	100	60%	11.2	1.08	2
2	0	100	77%	14.2	1.26	3
3	0	100	94%	17.8	1.32	5
4	-78	100	98%	18.6	1.15	40
5	-78	50	98%	9.2	1.12	30
6	-78	25	96%	4.4	1.16	20

^aPolymerizations were conducted with 4-methylbenzyl alcohol as the initiator and TBD as the catalyst in anhydrous dichloromethane at a monomer concentration of 2.0 M. ^bConversions (conv.) were obtained from ³¹P NMR spectra of aliquots taken from the polymerization mixtures. ^cM_{n, NMR} was determined by end-group analysis by ¹H NMR spectroscopy of the polymer. ^dĐ was measured by DMF SEC calibrated using polystyrene standards.

narrow Đ (1.1–1.2) was achieved at monomer conversions from 15 to 98%, indicating successful restriction of the side reactions.

The kinetics of polymerization were then studied in detail under these optimized conditions at -78 °C in the presence of 2 mol % TBD with a monomer concentration of 2.0 M in DCM and a monomer/initiator feed ratio ($[M]_0/[I]_0$) of 100. The linearity of M_n vs monomer conversion (Figure S2a) suggested that the numbers of growing macromolecules in the reactions remained constant during the polymerizations. Plots of ln($[M]_0/[M]$) vs time (Figure S2b) exhibited first-order kinetics, also suggesting the characteristics of a controlled polymerization. Further analysis by matrix-assisted laser desorption ionization time-of-flight mass spectrometry (MALDI-tof MS) of **6** (DP_n = 8 by ¹H NMR spectroscopy, Figure S3) revealed two populations, each with a spacing of 189 m/z, equal to that of the expected monomer repeat unit. Structurally, these two sets of signals were assigned to populations having the same end groups but distinct ionizations. The main peak in the major population at m/z = 1673 corresponded to a potassium-charged polymer chain of DP_n = 8 that had been initiated by 4-methylbenzyl alcohol and terminated by protonation, further confirming the controlled nature of the polymerization. Meanwhile, the main peak in the minor population at m/z = 1444 was in agreement with a proton-charged polymer chain of DP_n = 7 having 4-methylbenzyl oxy and protonated α- and ω-end groups, respectively.

By controlling the $[M]_0/[I]_0$ and the reaction time, a series of **6** with different molar masses were synthesized (ca. 2 to 18 kg/mol, Table 1 and Figure S2a). Across this range of molar masses, the polymers were soluble in common organic solvents but did not display water solubility. ³¹P NMR spectra clearly indicated two chemically distinct phosphorus environments, resonating at 9.88 and 9.04 ppm, corresponding to the chiral phosphorus atoms. ¹H NMR and ¹³C NMR spectra further confirmed the structure of **6**. Polymer **6** was a pale-yellow viscous liquid at room temperature and exhibited a glass transition temperature (T_g) of -12 to -8 °C (DP_n = 20–98). Compared to the T_g of -35 °C reported for an analogous polyphosphoester with alkyne side chains (DP_n = 50),^{15c} the T_g of **6** was higher, which was attributed to the phosphoramidate linkages along the polymer backbone. Yet, the T_g of **6** was significantly lower than that of **1** (DP_n = 20–93, T_g = 32–36

°C),¹³ likely due to the increased free volume provided by the larger butynyl side chains.

Having demonstrated that both **5** and **3** could undergo controlled ROPs under similar conditions to afford hydrophilic **1** and hydrophobic **6**, respectively, we then designed a synthetic route to produce amphiphilic diblock copolymers that would serve as acid-labile hosts for CPT in water. Given the high water solubility and hydrophilicity of **1**, it was expected that hydrophobic chain segments derived from **3** should be of greater relative length, to provide sufficient hydrophobicity to drive the assembly process and create a hydrophobic domain to maintain packaging of the drug molecules. After testing different block ratios, a 1:2 block ratio of PEOMP to PBYOMP was determined to yield aqueous assembly. The amphiphilic diblock copolymer **2** was obtained via one-pot sequential ROP of **5** and **3**, in which the sequence of the polymerization was the key to success (Scheme 1d). Due to the dilution of the solution mixture of the first block, the decreased concentration of the second monomer would likely result in a slower polymerization rate and lower polymerization conversion. The 2-fold amount of **3** used compared to **5** at this block ratio was also able to compensate for the dilution and be polymerized at the concentration of 2.0 M. Therefore, **3** was selected as the monomer for the second block, the higher activity of which further benefited these polymerizations. In contrast, selection of **5** as the second monomer suffered from dilution effects and resulted in lower than expected conversion (ca. 40%). Using an initially prepared **1** as a macroinitiator maintained as a reaction mixture at -78 °C, addition of **3** as a solution in DCM to afford a concentration of **3** at 2.0 M resulted in chain extension as observed by the peak in the SEC trace shifting toward shorter elution time relative to **1** (Figure S4). The increased molar mass as measured by SEC was consistent with the increased degree of polymerization determined by ¹H NMR spectroscopy. Although the molar mass distribution remained narrow (Đ < 1.2), indicative of a well-controlled polymerization, there was consistently a minor high molecular weight shoulder with several synthetic runs, which may be due to mixing complications because of the high viscosity of the polymerization mixture. To limit the breadth of the molar mass distribution and the presence of high molar mass impurities, the solution of monomer **3** was precooled to 0 °C and added as quickly as possible. This one-pot sequential synthesis of well-defined diblock PPAs provides several advantages over chain extension from purified macroinitiators, with fewer steps, shorter experimental time, and higher yields.

Aided by the hydrophilic PEOMP block, **2** dispersed readily into aqueous solution, while the alkynyl side chain groups on the hydrophobic PBYOMP block promoted assembly into core-shell micelles. CPT-loaded PPA nanoparticles (CPT@PPA) were prepared in a facile manner (Figure 1a), by dissolution of the polymer and CPT in ethanol, followed by removal of ethanol *in vacuo* and resuspension in nanopure water with sonication. The CPT concentration and loading capacity were optimized by tuning CPT and polymer concentrations. CPT loading was determined using high-performance liquid chromatography (HPLC), while the size and morphology of the loaded nanostructures were characterized by dynamic light scattering (DLS) and transmission electron microscopy (TEM). Preliminary experiments showed loading of CPT in the PPA nanoparticles of up to ca. 40 wt %, while for optimized stability of the system and inhibition of premature hydrolysis of CPT, a loading of 10 wt % was selected

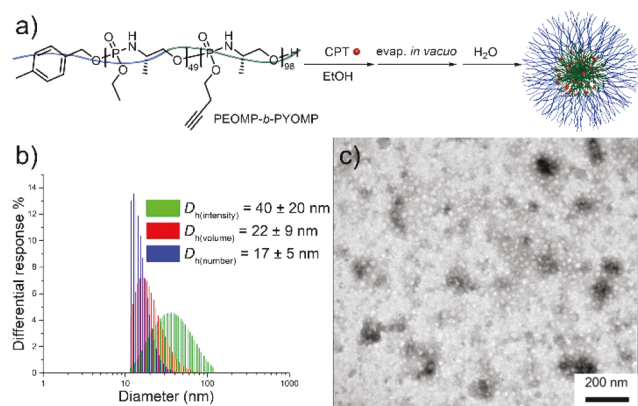


Figure 1. (a) Schematic representation of the formation of CPT@PPA by physical encapsulation of CPT into PPA. (b) Number-, intensity-, and volume-based hydrodynamic diameter distributions of CPT@PPA in nanopure water measured by DLS. (c) TEM images of CPT@PPA negatively stained by 1 wt % phosphotungstic acid aqueous solution (10 μ L), $D_{av} = 24 \pm 4$ nm (counting >50 nanoparticles). The dark spots are artifacts from phosphotungstic acid.

for morphological and biological characterization. DLS showed unimodal size distributions of the CPT@PPA nanocarriers, with a number-average hydrodynamic diameter ($D_{h(number)}$) of 17 ± 5 nm (Figure 1b). TEM images of CPT@PPA showed circular structures, with an average diameter (D_{av}) of 24 ± 4 nm (counting >50 nanoparticles, Figure 1c) suggesting the formation of micelles. The low T_g of PBYOMP ($DP_n = 20-98$, $T_g = -12$ to -8 °C) promoted flattening of the micellar structures in the dry state on TEM grids, leading to larger dry state diameters than those observed in solution.

The drug release profiles of CPT from CPT@PPA were measured in phosphate-buffered saline (PBS, pH 7.4) and citric acid- Na_2HPO_4 (pH 5.0) at 37 °C over 2.5 days. As depicted in Figure 2a, at pH 7.4, sustained release of CPT was observed over 2.5 days, while at pH 5.0, burst release of CPT was observed, with 98% of CPT released within 8 h. These distinct release profiles at different pH values are consistent with the acid-triggered degradation of the PPA backbone.¹³

The *in vitro* cytotoxicities of drug-equivalent loading CPT@PPA were investigated in three cancer and one noncancer cell lines and compared to cell viabilities for free CPT as a positive control with each cell line (Figure 2(b and c) and Table S1). The polymer micelles of 2 were found to be nontoxic at all concentrations tested (up to 175 μ g/mL). In human osteosarcoma cells (SJSA-1), CPT@PPA exhibited a lower IC_{50} (2.2 μ M) compared to free CPT (4.6 μ M), potentially indicating a protection against hydrolysis of CPT into the open, inactive carboxylate form. In addition, similarly lower IC_{50} values were observed for CPT@PPA in comparison to free CPT in human ovarian adenocarcinoma cells (OVCAR-3) and mouse leukemic monocyte-macrophage cells (RAW 264.7). In contrast, in mouse osteoblast precursor cells (MC3T3), IC_{50} values were not calculable up to the concentrations of CPT in both the CPT@PPA and free CPT formulations that had led to the cancer cell killing. Taken together, these studies demonstrate the advantages of CPT@PPA as anticancer agents, highlighting the potential for reduced side effects in healthy cells without sacrificing efficacy in cancer cells.

In summary, polymeric nanotherapeutics that display acid-triggered release were successfully obtained via the coassembly of PPA-based diblock copolymers and CPT into degradable,

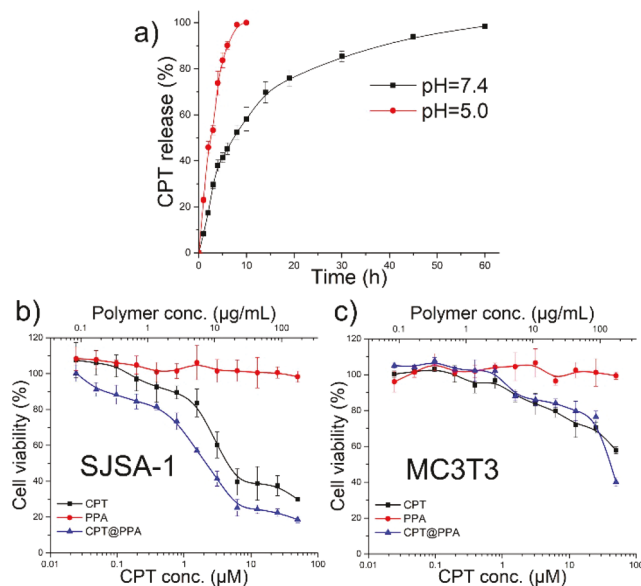


Figure 2. (a) Release of CPT from CPT@PPA (10 wt %) at pH 5.0 and pH 7.4 studied by a dialysis method over 2.5 days at 37 °C in citric acid- Na_2HPO_4 and PBS buffers, respectively, measured in triplicates. Cytotoxicity of CPT, PPA micelles, and CPT@PPA in (b) SJSA-1 and (c) MC3T3 cells. Cell viabilities are reported as an average of three measurements.

functional nanocarriers. An alkyne-functionalized oxazaphospholidine monomer was synthesized and polymerized in a controlled manner by its organobase-catalyzed ROP. One-pot sequential ROP yielded well-defined amphiphilic diblock polymers with acid-labile linkages along the backbone, good biocompatibility, and functionality. The alkyne-functionalized block provided both hydrophobicity to promote aqueous solution assembly and versatile reactive groups that allow for future manipulations, such as attachment of a dye and/or cross-linking of the core. Well-dispersed CPT-loaded nanoparticles with a $D_{h(number)}$ of 17 ± 5 nm were achieved through coassembly of the diblock copolymer with CPT, which exhibited sustained release of CPT at pH 7.4 and burst release at pH 5.0. Cytotoxicity assays demonstrated the biocompatibility of the polymer and enhanced efficacy of the CPT-loaded nanoparticles toward cancer cells, with minimal toxicity toward healthy cells. Future studies, including further modification of the polymer via alkyne groups and preparation of PPA-based nanoparticles loaded with different drugs, are underway.

ASSOCIATED CONTENT

Supporting Information

The Supporting Information is available free of charge on the ACS Publications website at DOI: 10.1021/acsmacrolett.8b00377.

Detailed experimental section, images, and tables (PDF)

AUTHOR INFORMATION

Corresponding Author

*(K.L.W.) E-mail: wooley@chem.tamu.edu. Tel.: (979) 845-4077.

ORCID

Hai Wang: 0000-0002-1215-2613

Karen L. Wooley: 0000-0003-4086-384X

Notes

The authors declare no competing financial interest.

ACKNOWLEDGMENTS

We gratefully acknowledge financial support from the National Science Foundation (NSF DMR-1507429 and NSF DMR-1309724) and from the Welch Foundation through the W. T. Doherty-Welch Chair in Chemistry (A-0001). Use of the TAMU/LBMS and the Texas A&M University Laboratory for Synthetic–Biologic Interactions is also acknowledged. Dr. Rachel A. Letteri is acknowledged for helpful discussions.

REFERENCES

- (1) (a) Kocak, G.; Tuncer, C.; Butun, V. pH-Responsive Polymers. *Polym. Chem.* **2017**, *8* (1), 144–176. (b) Zhang, S.; Bellinger, A. M.; Gletting, D. L.; Barman, R.; Lee, Y.-A. L.; Zhu, J.; Cleveland, C.; Montgomery, V. A.; Gu, L.; Nash, L. D.; Maitland, D. J.; Langer, R.; Traverso, G. A pH-Responsive Supramolecular Polymer Gel as an Enteric Elastomer for Use in Gastric Devices. *Nat. Mater.* **2015**, *14*, 1065.
- (2) Jochum, F. D.; Theato, P. Temperature- and Light-Responsive Smart Polymer Materials. *Chem. Soc. Rev.* **2013**, *42* (17), 7468–7483.
- (3) (a) Becker, G.; Marquetant, T. A.; Wagner, M.; Wurm, F. R. Multifunctional Poly(phosphoester)s for Reversible Diels–Alder Postmodification to Tune the LCST in Water. *Macromolecules* **2017**, *50* (20), 7852–7862. (b) Wolf, T.; Hunold, J.; Simon, J.; Rosenauer, C.; Hinderberger, D.; Wurm, F. R. Temperature Responsive Poly(phosphonate) Copolymers: From Single Chains to Macroscopic Coacervates. *Polym. Chem.* **2018**, *9* (4), 490–498. (c) Hearon, K.; Wierzbicki, M. A.; Nash, L. D.; Landsman, T. L.; Laramy, C.; Lonneck, A.T.; Gibbons, M. C.; Ur, S.; Cardinal, K. O.; Wilson, T. S.; Wooley, K. L.; Maitland, D. J. A Processable Shape Memory Polymer System for Biomedical Applications. *Adv. Healthcare Mater.* **2015**, *4* (9), 1386–1398.
- (4) Zhang, X.; Han, L.; Liu, M.; Wang, K.; Tao, L.; Wan, Q.; Wei, Y. Recent Progress and Advances in Redox-Responsive Polymers as Controlled Delivery Nanoplatfoms. *Mater. Chem. Front.* **2017**, *1* (5), 807–822.
- (5) Ge, J.; Neofytou, E.; Cahill, T. J.; Beygui, R. E.; Zare, R. N. Drug Release from Electric-Field-Responsive Nanoparticles. *ACS Nano* **2012**, *6* (1), 227–233.
- (6) Mura, S.; Nicolas, J.; Couvreur, P. Stimuli-Responsive Nanocarriers for Drug Delivery. *Nat. Mater.* **2013**, *12*, 991.
- (7) (a) Su, L.; Li, R.; Khan, S.; Clanton, R.; Zhang, F.; Lin, Y.-N.; Song, Y.; Wang, H.; Fan, J.; Hernandez, S.; Butters, A. S.; Akabani, G.; MacLoughlin, R.; Smolen, J.; Wooley, K. L. Chemical Design of Both a Glutathione-Sensitive Dimeric Drug Guest and a Glucose-Derived Nanocarrier Host to Achieve Enhanced Osteosarcoma Lung Metastatic Anticancer Selectivity. *J. Am. Chem. Soc.* **2018**, *140* (4), 1438–1446. (b) Zhang, F.; Gong, S.; Wu, J.; Li, H.; Oupicky, D.; Sun, M. CXCR4-Targeted and Redox Responsive Dextrin Nanogel for Metastatic Breast Cancer Therapy. *Biomacromolecules* **2017**, *18* (6), 1793–1802. (c) Zhong, P.; Meng, H.; Qiu, J.; Zhang, J.; Sun, H.; Cheng, R.; Zhong, Z. $\alpha_3\beta_1$ Integrin-Targeted Reduction-Sensitive Micellar Mertansine Prodrug: Superb Drug Loading, Enhanced Stability, and Effective Inhibition of Melanoma Growth In Vivo. *J. Controlled Release* **2017**, *259*, 176–186. (d) Zhu, A.; Miao, K.; Deng, Y.; Ke, H.; He, H.; Yang, T.; Guo, M.; Li, Y.; Guo, Z.; Wang, Y.; Yang, X.; Zhao, Y.; Chen, H. Dually pH/Reduction-Responsive Vesicles for Ultrahigh-Contrast Fluorescence Imaging and Thermo-Chemotherapy-Synergized Tumor Ablation. *ACS Nano* **2015**, *9* (8), 7874–7885. (e) Li, H.-J.; Du, J.-Z.; Du, X.-J.; Xu, C.-F.; Sun, C.-Y.; Wang, H.-X.; Cao, Z.-T.; Yang, X.-Z.; Zhu, Y.-H.; Nie, S.; Wang, J. Stimuli-Responsive Clustered Nanoparticles for Improved Tumor Penetration and Therapeutic Efficacy. *Proc. Natl. Acad. Sci. U. S. A.* **2016**, *113* (15), 4164–4169. (f) Jiang, X.; Zheng, Y.; Chen, H. H.; Leong, K. W.; Wang, T. H.; Mao, H. Q. Dual-Sensitive Micellar Nanoparticles Regulate DNA Unpacking and Enhance Gene-Delivery Efficiency. *Adv. Mater.* **2010**, *22* (23), 2556–2560.
- (8) (a) Li, H.-J.; Du, J.-Z.; Liu, J.; Du, X.-J.; Shen, S.; Zhu, Y.-H.; Wang, X.; Ye, X.; Nie, S.; Wang, J. Smart Superstructures with Ultrahigh pH-Sensitivity for Targeting Acidic Tumor Microenvironment: Instantaneous Size Switching and Improved Tumor Penetration. *ACS Nano* **2016**, *10* (7), 6753–6761. (b) Xu, X.; Wu, J.; Liu, Y.; Yu, M.; Zhao, L.; Zhu, X.; Bhasin, S.; Li, Q.; Ha, E.; Shi, J.; Farokhzad, O. C. Ultra-pH-Responsive and Tumor-Penetrating Nanoplatform for Targeted siRNA Delivery with Robust Anti-Cancer Efficacy. *Angew. Chem., Int. Ed.* **2016**, *55* (25), 7091–7094. (c) Yang, G.; Xu, L.; Xu, J.; Zhang, R.; Song, G.; Chao, Y.; Feng, L.; Han, F.; Dong, Z.; Li, B.; Liu, Z. Smart Nanoreactors for pH-Responsive Tumor Homing, Mitochondria-Targeting, and Enhanced Photodynamic-Immunotherapy of Cancer. *Nano Lett.* **2018**, *18* (4), 2475–2484. (d) Yu, H.; Cui, Z.; Yu, P.; Guo, C.; Feng, B.; Jiang, T.; Wang, S.; Yin, Q.; Zhong, D.; Yang, X.; Zhang, Z.; Li, Y. pH- and NIR Light-Responsive Micelles with Hyperthermia-Triggered Tumor Penetration and Cytoplasm Drug Release to Reverse Doxorubicin Resistance in Breast Cancer. *Adv. Funct. Mater.* **2015**, *25* (17), 2489–2500. (e) Li, J.; Li, Y.; Wang, Y.; Ke, W.; Chen, W.; Wang, W.; Ge, Z. Polymer Prodrug-Based Nanoreactors Activated by Tumor Acidity for Orchestrated Oxidation/Chemotherapy. *Nano Lett.* **2017**, *17* (11), 6983–6990.
- (9) (a) Selvi, B.; Patel, S.; Savva, M. Physicochemical Characterization and Membrane Binding Properties of Camptothecin. *J. Pharm. Sci.* **2008**, *97* (10), 4379–4390. (b) Pommier, Y. Topoisomerase I Inhibitors: Camptothecins and Beyond. *Nat. Rev. Cancer* **2006**, *6*, 789.
- (10) (a) Cai, K.; He, X.; Song, Z.; Yin, Q.; Zhang, Y.; Uckun, F. M.; Jiang, C.; Cheng, J. Dimeric Drug Polymeric Nanoparticles with Exceptionally High Drug Loading and Quantitative Loading Efficiency. *J. Am. Chem. Soc.* **2015**, *137* (10), 3458–3461. (b) Jin, H.; Sun, M.; Shi, L.; Zhu, X.; Huang, W.; Yan, D. Reduction-Responsive Amphiphilic Polymeric Prodrugs of Camptothecin-Polyphosphoester for Cancer Chemotherapy. *Biomater. Sci.* **2018**, *6*, 1403. (c) Hu, M.; Huang, P.; Wang, Y.; Su, Y.; Zhou, L.; Zhu, X.; Yan, D. Synergistic Combination Chemotherapy of Camptothecin and Floxuridine through Self-Assembly of Amphiphilic Drug–Drug Conjugate. *Bioconjugate Chem.* **2015**, *26* (12), 2497–2506. (d) Xu, Z.; Wang, D.; Xu, S.; Liu, X.; Zhang, X.; Zhang, H. Preparation of a Camptothecin Prodrug with Glutathione-Responsive Disulfide Linker for Anticancer Drug Delivery. *Chem. - Asian J.* **2014**, *9* (1), 199–205. (e) Zhang, Q.; He, J.; Zhang, M.; Ni, P. A Polyphosphoester-Conjugated Camptothecin Prodrug with Disulfide Linkage for Potent Reduction-Triggered Drug Delivery. *J. Mater. Chem. B* **2015**, *3* (24), 4922–4932. (f) McRae Page, S.; Martorella, M.; Parelkar, S.; Kosif, I.; Emrick, T. Disulfide Cross-Linked Phosphorylcholine Micelles for Triggered Release of Camptothecin. *Mol. Pharmaceutics* **2013**, *10* (7), 2684–2692. (g) Hu, X.; Hu, J.; Tian, J.; Ge, Z.; Zhang, G.; Luo, K.; Liu, S. Polyprodrug Amphiphiles: Hierarchical Assemblies for Shape-Regulated Cellular Internalization, Trafficking, and Drug Delivery. *J. Am. Chem. Soc.* **2013**, *135* (46), 17617–17629.
- (11) (a) Min, K. H.; Kim, J.-H.; Bae, S. M.; Shin, H.; Kim, M. S.; Park, S.; Lee, H.; Park, R.-W.; Kim, I.-S.; Kim, K.; Kwon, I. C.; Jeong, S. Y.; Lee, D. S. Tumoral Acidic pH-Responsive MPEG-Poly(β -amino ester) Polymeric Micelles for Cancer Targeting Therapy. *J. Controlled Release* **2010**, *144* (2), 259–266. (b) Hu, X.; Li, H.; Luo, S.; Liu, T.; Jiang, Y.; Liu, S. Thiol and pH Dual-Responsive Dynamic Covalent Shell Cross-Linked Micelles for Triggered Release of Chemotherapeutic Drugs. *Polym. Chem.* **2013**, *4* (3), 695–706.
- (12) Li, L.; Xu, Y.; Milligan, I.; Fu, L.; Franckowiak, E. A.; Du, W. Synthesis of Highly pH-Responsive Glucose Poly(orthoester). *Angew. Chem., Int. Ed.* **2013**, *52* (51), 13699–13702.
- (13) Wang, H.; Su, L.; Li, R.; Zhang, S.; Fan, J.; Zhang, F.; Nguyen, T. P.; Wooley, K. L. Polyphosphoramidates That Undergo Acid-Triggered Backbone Degradation. *ACS Macro Lett.* **2017**, *6* (3), 219–223.
- (14) (a) Zhang, S.; Wang, H.; Shen, Y.; Zhang, F.; Seetho, K.; Zou, J.; Taylor, J.-S. A.; Dove, A. P.; Wooley, K. L. A Simple and Efficient Synthesis of an Acid-Labile Polyphosphoramidate by Organobase-

Catalyzed Ring-Opening Polymerization and Transformation to Polyphosphoester Ionomers by Acid Treatment. *Macromolecules* **2013**, *46* (13), 5141–5149. (b) Nifant'ev, I. E.; Shlyakhtin, A. V.; Bagrov, V. V.; Komarov, P. D.; Kosarev, M. A.; Tavtorkin, A. N.; Minyaev, M. E.; Roznyatovsky, V. A.; Ivchenko, P. V. Controlled Ring-Opening Polymerisation of Cyclic Phosphates, Phosphonates and Phosphoramidates Catalysed by Heteroleptic BHT-Alkoxy Magnesium Complexes. *Polym. Chem.* **2017**, *8* (44), 6806–6816.

(15) (a) Su, L.; Khan, S.; Fan, J.; Lin, Y.-N.; Wang, H.; Gustafson, T. P.; Zhang, F.; Wooley, K. L. Functional Sugar-Based Polymers and Nanostructures Comprised of Degradable Poly(D-glucose carbonate)s. *Polym. Chem.* **2017**, *8*, 1699–1707. (b) Iwasaki, Y.; Yokota, A.; Otake, A.; Inoue, N.; Yamaguchi, A.; Yoshitomi, T.; Yoshimoto, K.; Neo, M. Bone-Targeting Poly(ethylene sodium phosphate). *Biomater. Sci.* **2018**, *6* (1), 91–95. (c) Zhang, S.; Li, A.; Zou, J.; Lin, L. Y.; Wooley, K. L. Facile Synthesis of Clickable, Water-Soluble, and Degradable Polyphosphoesters. *ACS Macro Lett.* **2012**, *1* (2), 328–333.

(16) (a) Bauer, K. N.; Liu, L.; Andrienko, D.; Wagner, M.; Macdonald, E. K.; Shaver, M. P.; Wurm, F. R. Polymerizing Phostones: A Fast Way to in-Chain Poly(phosphonate)s with Adjustable Hydrophilicity. *Macromolecules* **2018**, *51* (4), 1272–1279. (b) Zhang, F.; Smolen, J. A.; Zhang, S.; Li, R.; Shah, P. N.; Cho, S.; Wang, H.; Raymond, J. E.; Cannon, C. L.; Wooley, K. L. Degradable Polyphosphoester-Based Silver-Loaded Nanoparticles as Therapeutics for Bacterial Lung Infections. *Nanoscale* **2015**, *7* (6), 2265–2270.